CellPress

Structure
Article

Structural Basis for the Inhibition of Host Protein Ubiquitination by *Shigella* Effector Kinase OspG

Andrey M. Grishin,[1] Tara E.C. Condos,[2] Kathryn R. Barber,[2] François-Xavier Campbell-Valois,[3,4] Claude Parsot,[3,4] Gary S. Shaw,[2] and Miroslaw Cygler[1,5,*]
[1]Department of Biochemistry, University of Saskatchewan, 107 Wiggins Road, Saskatoon, SK S7N 5E5, Canada
[2]Department of Biochemistry, University of Western Ontario, London, ON N6A 5C1, Canada
[3]Unité de Pathogénie Microbienne Moléculaire, Institut Pasteur, 75724 Paris, France
[4]INSERM, U786, 75015, Paris, France
[5]Department of Biochemistry, McGill University, Montreal, QC H3G 1Y6, Canada
*Correspondence: miroslaw.cygler@usask.ca
http://dx.doi.org/10.1016/j.str.2014.04.010

SUMMARY

Shigella **invasion of its human host is assisted by T3SS-delivered effector proteins. The OspG effector kinase binds ubiquitin and ubiquitin-loaded E2-conjugating enzymes, including UbcH5b and UbcH7, and attenuates the host innate immune NF-kB signaling. We present the structure of OspG bound to the UbcH7∼Ub conjugate. OspG has a minimal kinase fold lacking the activation loop of regulatory kinases. UbcH7∼Ub binds OspG at sites remote from the kinase active site, yet increases its kinase activity. The ubiquitin is positioned in the "open" conformation with respect to UbcH7 using its I44 patch to interact with the C terminus of OspG. UbcH7 binds to OspG using two conserved loops essential for E3 ligase recruitment. The interaction of the UbcH7∼Ub with OspG is remarkably similar to the interaction of an E2∼Ub with a HECT E3 ligase. OspG interferes with the interaction of UbcH7 with the E3 parkin and inhibits the activity of the E3.**

INTRODUCTION

Shigella is a Gram-negative pathogenic bacterium causing destruction of the intestinal mucosa and dysentery in humans. As with other Gram-negative pathogens, such as *Salmonella*, pathogenic *Escherichia coli*, and *Yersinia*, *Shigella* utilizes a type III secretion system (T3SS) (Worrall et al., 2011) to deliver over 20 effector proteins into host cells (Buchrieser et al., 2000). These effectors hijack cellular processes of the host to promote invasion, survival, and proliferation of bacteria (Dean, 2011).

Phosphorylation plays a central role in cellular signaling with over 500 kinases encoded in mammalian genomes (Manning et al., 2002). Some T3SS effectors, such as SteC (*Salmonella*) (Poh et al., 2008), LegKs (*Legionella*) (Ge et al., 2009), and YpkA (*Yersinia*) (Wiley et al., 2009), show high sequence similarity to human kinases and were likely acquired via horizontal gene transfer. Other T3SS effectors, such as OspG (*Shigella*) (Kim et al., 2005; Zhou et al., 2013), NleHs (pathogenic *E. coli*) (Gao et al., 2009), SboH (*Salmonella*), and YspK (*Yersinia*) (Matsumoto and Young, 2006) are only distantly related to mammalian kinases (Kannan et al., 2007). The effector OspG is composed of a kinase-like domain and an N-terminal T3SS secretion signal (Kim et al., 2005; Zhou et al., 2013). Using a yeast two-hybrid system, Kim et al. (2005) identified the ubiquitin-conjugating enzymes (E2s) UbcH5b, UbcH5c, UbcH7, UbcH8, UbcH9, and RIG-B as OspG interactors. Pull-down experiments showed that binding to OspG was only observed when the E2 was conjugated to ubiquitin (Ub). Expression of OspG in HEK293T cells prevented the proteasome-dependent degradation of phospho-IκBα, the inhibitor of the NF-κB pathway. This effect was dependent upon the kinase activity of OspG (Kim et al., 2005); however, the phosphorylation targets of OspG have not been identified. Kim et al. (2005) hypothesized that the UbcH5b∼Ub conjugate serves to "shuttle" OspG to the $SCF^{\beta-TrCP}$ complex to phosphorylate some of its components and inhibit its activity. More recently, Zhou et al. (2013) showed that OspG also binds ubiquitin and polyubiquitin chains and that this binding stimulates its kinase activity.

E2-conjugating proteins are the central enzymes in the ubiquitination pathway. They accept an Ub from an E1 enzyme and transfer it either directly to a substrate using a scaffolding *r*eally *i*nteresting *n*ew *g*ene (RING) E3 ligase or via the formation of a thioester bond with a *h*omologous to *E*6AP *C* *t*erminus (HECT) E3 ligase. The smaller class of RBR E3 ligases uses a hybrid mechanism that has aspects of both RING and HECT mechanisms (Wenzel et al., 2011). Ubiquitination proceeds in a stepwise process with the formation of an E1:E2 complex to transfer Ub from the E1 to an E2 and the formation of an E2:E3 complex to transfer Ub either directly to a substrate with the help of a RING E3 or to a HECT E3. Structural studies have revealed that E2s use similar regions to recruit both the E1 and E3s (van Wijk and Timmers, 2010). In E2:E3 complexes, the relative positions of the E2 and Ub ("open," "closed," or "backbent") are dictated by the E2:E3 pair (Page et al., 2012). In the HECT E3 NEDD4L:UbcH5b∼Ub complex (Protein Data Bank [PDB] ID code 3JW0) (Kamadurai et al., 2009) Ub is in the "open" state; there is little contact between the E2 and Ub, which are in an

extended configuration when recruited to the E3. In the RING E3 RNF4:UbcH5A∼Ub (PDB ID code 4AP4) (Plechanovová et al., 2012) and RING E3 BIRC7:UbcH5B∼Ub (PDB ID code 4AUQ) (Dou et al., 2012) complexes, Ub is in a "closed" conformation; Ub interacts with a portion of E2 to form a more contiguous surface to recruit the E3.

The observations that OspG is endowed with a kinase activity and can interact with Ub and several E2∼Ub conjugates, such as UbcH7 and UbcH5b, suggest that OspG might interfere with the ubiquitin-dependent degradation pathway and raise several questions: (1) are E2∼Ub conjugates, Ub/poly-Ub, or both the biologically relevant partners of OspG; (2) how does the binding of an E2∼Ub conjugate affect the kinase activity of OspG and alter the ubiquitination process to prevent activation of the NF-κB pathway; and (3) what might be the target of the kinase activity. To address these issues, we determined the crystal structure of the complex of OspG with the UbcH7∼Ub conjugate in the absence and in the presence of an ATP analog. The structures show that the OspG:UbcH7∼Ub interface does not occlude the active site on OspG, providing an explanation for the observed kinase activity in the presence of the conjugate or ubiquitin. Affinity measurements indicated that OspG interacts with the UbcH7∼Ub conjugate 15-fold tighter than with Ub alone, suggesting that the E2∼Ub conjugate is the most relevant cellular binding partner of OspG. In the complex, Ub is in an "open" position with respect to UbcH7, as observed in the UbcH5b∼Ub complex associated with the HECT E3 NEDD4L. Crucially, UbcH7 binds OspG through the same region that is used to recruit an E3 prior to Ub transfer to a substrate. Using in vitro ubiquitination assays, we demonstrated that ubiquitination by the E3 parkin is attenuated in the presence of OspG. These structural and biochemical results suggest a mechanism by which OspG might interfere with the ubiquitination machinery.

RESULTS

OspG Preferentially Interacts with the UbcH7∼Ub Conjugate

Kim et al. (2005) showed that OspG interacts with several E2-conjugating enzymes in their Ub-loaded forms only. Recently, Zhou et al. (2013) showed that OspG also binds Ub. To investigate the interactions between OspG and UbcH7, Ub, and the UbcH7∼Ub conjugate, we used (1) a stable E2∼Ub complex formed by a disulfide linkage between the C terminus of Ub (G76C) and the catalytic cysteine (C86) in UbcH7 (Serniwka and Shaw, 2009) and (2) an OspG protein lacking the N-terminal 25 residues, as this portion of the protein represents the T3SS secretion signal and is not important for Ub binding or kinase function (Zhou et al., 2013). To dissect the relative contributions of UbcH7 and Ub in OspG recruitment, we quantified the interactions of OspG with UbcH7, Ub, and the UbcH7∼Ub conjugate using NMR spectroscopy, isothermal titration calorimetry (ITC), and size-exclusion chromatography (SEC).

Initial NMR experiments were used to monitor the interaction of Ub and UbcH7 within the UbcH7∼Ub conjugate, in which only UbcH7 was ^{15}N labeled. The ^{1}H-^{15}N HSQC spectrum of UbcH7 within the conjugate showed that only the amide resonances for residues Cys86 and Leu87 were shifted with respect to their positions in UbcH7 alone (Figure S1A available online), indicating that the UbcH7∼Ub complex is intact. The lack of obvious changes in the remainder of the UbcH7 spectrum in the UbcH7∼Ub conjugate also showed that minimal contacts exist between the E2 and Ub in solution. Addition of OspG to UbcH7∼Ub resulted in a significant broadening of a large number of signals, indicative of the formation of a complex between OspG and UbcH7∼Ub (46.2 kDa). Similar experiments were performed using ^{15}N-labeled UbcH7 or ^{15}N-labeled Ub to examine the individual interactions of each of these proteins with OspG. Addition of unlabeled OspG to ^{15}N-labeled UbcH7 revealed minor changes in chemical shifts, indicative of a very weak interaction. In contrast, addition of unlabeled OspG to ^{15}N-labeled Ub resulted in shifting or broadening of several resonances, including Thr7, Leu8, Arg48, Gln49, His68, Leu69, and Val70 (Figure S1B), identifying an interaction site near the classic I44 patch of ubiquitin and confirming the interaction of OspG with Ub observed previously (Zhou et al., 2013).

The strength of the interaction between OspG and UbcH7∼Ub, Ub, and UbcH7 was quantified using isothermal titration calorimetry. The interaction between OspG and UbcH7∼Ub displayed a dissociation constant K_d of 580 ± 20 nM at 25°C. In contrast, the interactions of OspG with Ub (K_d 9 ± 0.4 μM) and UbcH7 (K_d ∼90 μM) were about 15 and 150 times weaker (Figure 1). These results were confirmed by size-exclusion chromatography, which was able to detect the complex of OspG with the UbcH7∼Ub conjugate, but not with UbcH7 or Ub alone. Addition of a reducing agent to the OspG:UbcH7∼Ub complex prior to gel filtration caused OspG, UbcH7, and Ub to elute as separate peaks (Figure S2). Together, these results demonstrated a strong preference for the recruitment of OspG to an E2-Ub conjugate rather than to individual Ub or UbcH7 components.

The Structure of the OspG:UbcH7∼Ub Complex

OspG Structure

The structure of the OspG:UbcH7∼Ub complex was determined with and without a nucleotide analog (Figure 2; Table 1). As expected from previous biochemical data (Kim et al., 2005; Zhou et al., 2013), OspG has a kinase-like fold, although it lacks several elements of the canonical kinases (Figures 2B and 2C). Its structure represents a minimal kinase domain, comprising segments I–VII and IX of the classical regulatory kinase fold (Hanks and Hunter, 1995). In the complex, OspG consists of two subdomains with an active center situated in a deep cleft between them. The N-terminal subdomain (N-lobe, residues 26–101) is built of a five-stranded β sheet (β1–β5) and a helix α1 (segments I–IV) (Figure 2B) and includes a Gly-rich P loop (segment I) with the sequence I^{33}GQGSTAEI^{41}, the invariant Lys53 (segment II), and Glu72 (helix α1, frequently called α helix C, segment III). The P loop participates in ATP binding, whereas Lys53 participates in the orientation of ATP β- and γ-phosphate groups. The carboxyl group of Glu72 forms a hydrogen bond with the amine group of Lys53, properly positioning this side chain for catalysis. The C-terminal subdomain (C-lobe, residues 102–196) has a mixed α/β fold with two β strands (β6, β7), two long helices (α3, α4), and two one-turn helices (α2, α3′) (segments V–VII, IX) (Figure 2B). It contains the "catalytic loop" (segment VIB) with the sequence HY**D**^{138}LNTG**N**^{143} differing from the consensus sequence $^{H}/_{Y}$RDX$^{K}/_{X}$XXN of human kinases (Hanks and Hunter, 1995). The conserved DFG motif in segment

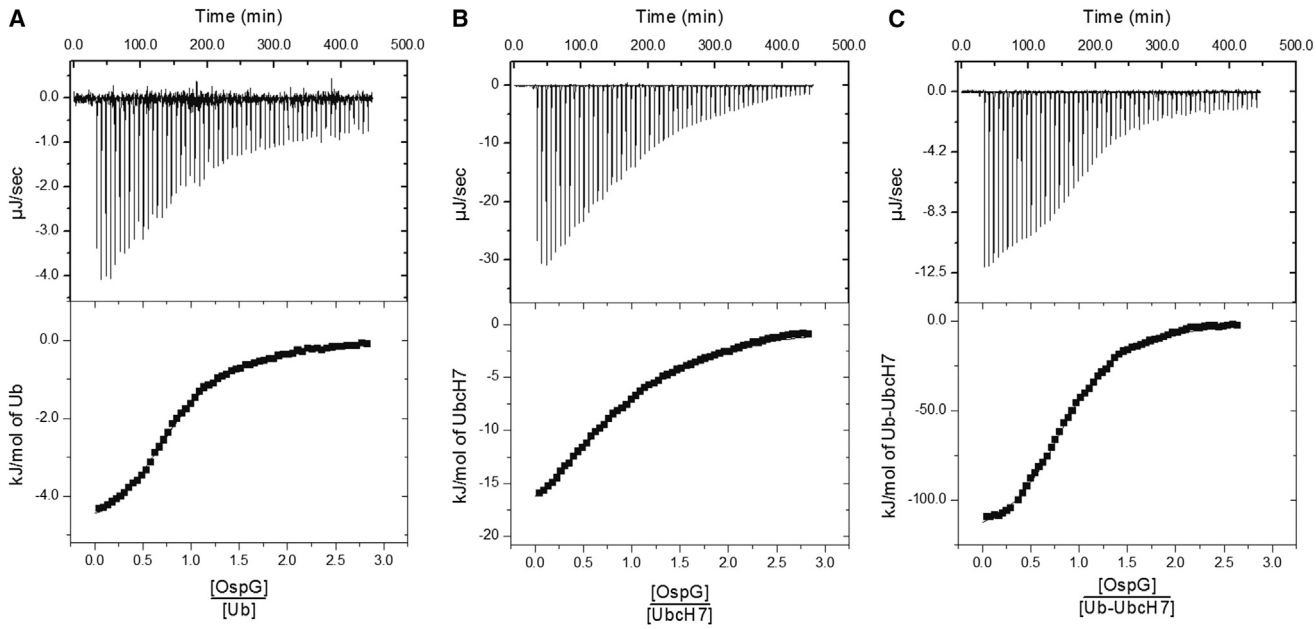

Figure 1. Isothermal Titration Calorimetry Analysis for OspG Binding to Ub, UbcH7, and UbcH7∼Ub

(A) Isotherm graph for OspG and Ub.

(B) Isotherm graph for OspG and UbcH7.

(C) Isotherm graph for OspG and UbcH7∼Ub.

The upper panels present raw data, and the lower panels present the integrated heat changes for a single-site binding model. Data were collected in buffers containing 100 mM Na H_2PO_4, 100 mM NaCl (pH 7.5) at 25°C.

VII is replaced in OspG by the **D**^{157}FR sequence. Segment VIII, corresponding to the activation loop in regulatory kinases, is significantly shorter and is followed by the C-terminal helix α4 (also called α helix F, segment IX).

A comparison with the structures of typical regulatory kinases indicates that OspG assumes an active conformation in the complex; the seven catalytically important residues (Gly34, Gly36, Lys53, Glu72, Asp138, Asn143, and Asp157) superimpose on the corresponding residues of the active state of protein kinase A (PKA; PDB ID code 1ATP) with a root-mean-square deviation (rmsd) of 0.8 Å for all Cα atoms (Figure 2C). Additionally, the conformation of the conserved D^{157}FR motif is also typical of the active state of the regulatory kinases. Moreover, the so-called "regulatory" (R) and "catalytic" (C) spines, present only in the active states of regulatory kinases (Kornev et al., 2006, 2008), are fully assembled in OspG (Figure S3A). The structure of OspG is similar to the recently determined structures of NleH1/2 kinase domains with the exception of the placement of helix α4 in segment IX (Grishin et al., 2014) (Figure S3B). The superposition of these molecules results in an rmsd of 1.28 Å for 115 Cα atoms out of 168 (excluding α4 and a few loops).

ATP Binding and the Active Site

Comparison of OspG:UbcH7∼H7 complexes obtained in the absence and in the presence of AMPPNP showed that the nucleotide binding proceeds with minimal structural adjustments—0.3 Å rmsd for all atoms of the seven key active site residues (excluding Asp157 sidechain that adopts different conformation) (Figure 2D). The adenine moiety binds within a conserved hydrophobic pocket composed of Ile41, Leu51, Phe76, Met98, Val101, Leu145, and Ile156, with an amino group pointing toward the bottom of the pocket and forming a hydrogen bond with the backbone carbonyl of Leu99, whereas the adenine N7 hydrogen bonds to the amide of Asp157 through a bridging water. Although OspG differs in four out of seven residues defining the adenine pocket from PKA, the hydrophobicity of the pocket is well preserved and the nucleotide binding mode is very similar in the two proteins. The α-phosphate in AMPPNP makes a hydrogen bond with Lys53, an essential residue for the kinase activity (Kim et al., 2005; Zhou et al., 2013), whereas the γ-phosphate interacts with Asn143 and Asp157. The Mg^{2+} ion is coordinated in a tetragonal bipyramid with the carboxyl group of Asp157 and several water molecules and corresponds to the primary Mg^{2+} atom in PKA. The γ-phosphate in OspG occupies the position of the secondary Mg^{2+} in PKA.

Interaction of Ub with OspG

The structure of OspG:UbcH7∼Ub shows atomic details of the adaptation of a minimal-fold kinase to the binding of a relatively large molecular complex through multiple interfaces. Mutational analysis identified the C terminus of OspG as essential for Ub binding (Zhou et al., 2013); however, the detailed molecular nature of this interaction has not been determined. Our structural analysis shows that Ub binds to a hydrophobic depression between α3 and α4 near the C terminus of OspG. This depression is created through a different placement of α4 (helix F, segment IX) in OspG with respect to its counterparts in PKA (Figure 2C) and NleH1/2 (Figure S3B). Further, whereas the C terminus of α4 is in a similar position to that in PKA, anchored via Phe187 and Leu190 to the C-spine of OspG, the N-terminal part is shifted by ∼7 Å and occupies a position taken by the activation loop in the active state of PKA. The repositioning of these two helices in

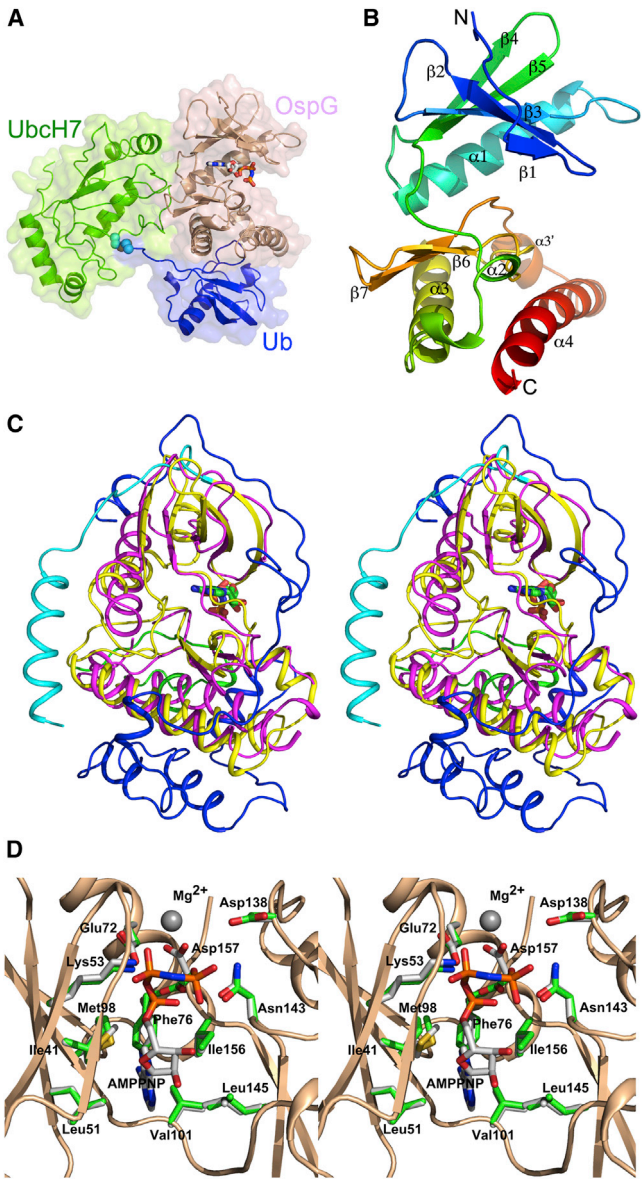

Figure 2. Structure of OspG:UbcH7∼Ub Complex

(A) The view of the complex corresponds to a standard kinase orientation with the helical domain at the bottom, sheet domain at the top, and the substrate binding site on the right. The proteins are shown in cartoon form. OspG is colored in wheat; UbcH7 is in green; and Ub is in blue. The solvent-accessible surface is shown as semitransparent. The ATP analog AMPPNP (red) is shown in the active site of OspG. The Cys86 (UbcH7) and Cys76 (Ub) residues participating in the disulfide bond formation are shown as spheres.

(B) OspG cartoon drawing with marked secondary structures. The molecule is painted in rainbow colors, from blue at the N terminus to red at the C terminus.

(C) Comparison of the OspG structure with the canonical regulatory kinase fold of protein kinase A (PKA). OspG is colored magenta, whereas PKA is colored according to its core (yellow), activation loop (green), N-terminal extension (cyan), and C-terminal extension (blue) regions. The AMPPNP nucleotide (shown as sticks) marks the location of the active site.

(D) The active-site region of OspG with (white) and without (green) nucleotide. Only Asp157 changes orientation upon nucleotide binding.

Table 1. Summary of Data Collection and Refinement Statistics

Data Set	OspG+UbcH7∼Ub	OspG+UbcH7 ∼Ub+AMPPNP
Space group	$P2_12_12_1$	$P2_12_12_1$
a,b,c (Å)	67.3, 84.1, 85.4	67.4, 84.7, 85.9
α,β,γ (°)	90, 90, 90	90, 90, 90
Wavelength (Å)	0.97949	0.97949
Resolution (Å)	50.0–1.87	50.0–2.0
Last resolution shell (Å)	1.9–1.87	2.03–2.0
Observed hkl	449,840	242,414
Unique hkl	40,758	33,962
Completeness (%)[a]	100.0 (100.0)	99.9 (100.0)
Redundancy[a]	11.0 (11.1)	7.1 (7.0)
Rsym[a]	10.0 (>1.00)	9.4 (>1.00)
I/(σI)[a]	30.5 (2.0)	25.5 (1.98)
R_{work}	20.27	20.24
R_{free} (%hkl)	24.29 (5)	24.3 (5)
Wilson B (Å^2)	35.6	35.07
B-Factor Å^2 (no. of atoms)		
Protein	55.7 (3,256)	43.4 (3,285)
Solvent	47.2 (237)	33.4 (212)
Ligand	NA	29.2 (33)
Ramachandran Plot		
Allowed (%)	97.67	97.12
Generous (%)	2.07	2.62
Disallowed (%)	0.26	0.26
Rmsd		
Bonds (Å)	0.006	0.008
Angles (°)	0.98	1.18
PDB ID codes	4Q5E	4Q5H

[a]The information for the last shell of resolution is given in parentheses.

OspG, relative to that observed in other kinases, creates the hydrophobic depression used as the focal point for Ub binding. Ub contacts OspG through residues from its four β strands and the loop following β4. The turn between β3 and β4 (Ala46-Gly47-Arg48) protrudes into the center of the OspG depression created by α3 and α4 approaching His136 (R-spine) in the HY**D**^{138}LNTG**N**^{143} motif of OspG (Figure 3A). The Ub residues Leu8, Ile44, and Val70 used to recruit OspG, form a hydrophobic patch well known for involvement in Ub binding to other proteins (Beal et al., 1998; Sloper-Mould et al., 2001; Lee et al., 2006). Other Ub residues contacting OspG, such as Arg48, Gln49, Glu51, Arg54, Ser57, Asp58, and Tyr59, have a more polar nature. For example, hydrogen bonds from Glu51 in Ub are formed to Asn130 and Tyr162 in OspG, whereas Tyr59 in Ub forms herringbone contacts to Tyr165 and Tyr166 in OspG. In addition, Arg48 in Ub (Lys48 in wild-type Ub) forms a salt bridge with Asp177 in OspG (Figure S4A).

Interaction of OspG with UbcH7

Whereas Ub binds to the C-lobe of OspG away from the OspG substrate binding site, UbcH7 contacts both the N- and C-lobes on the backside of OspG (Figure 2A). The OspG surface binding UbcH7 is relatively flat, hydrophobic in the center (Phe79, Tyr80,

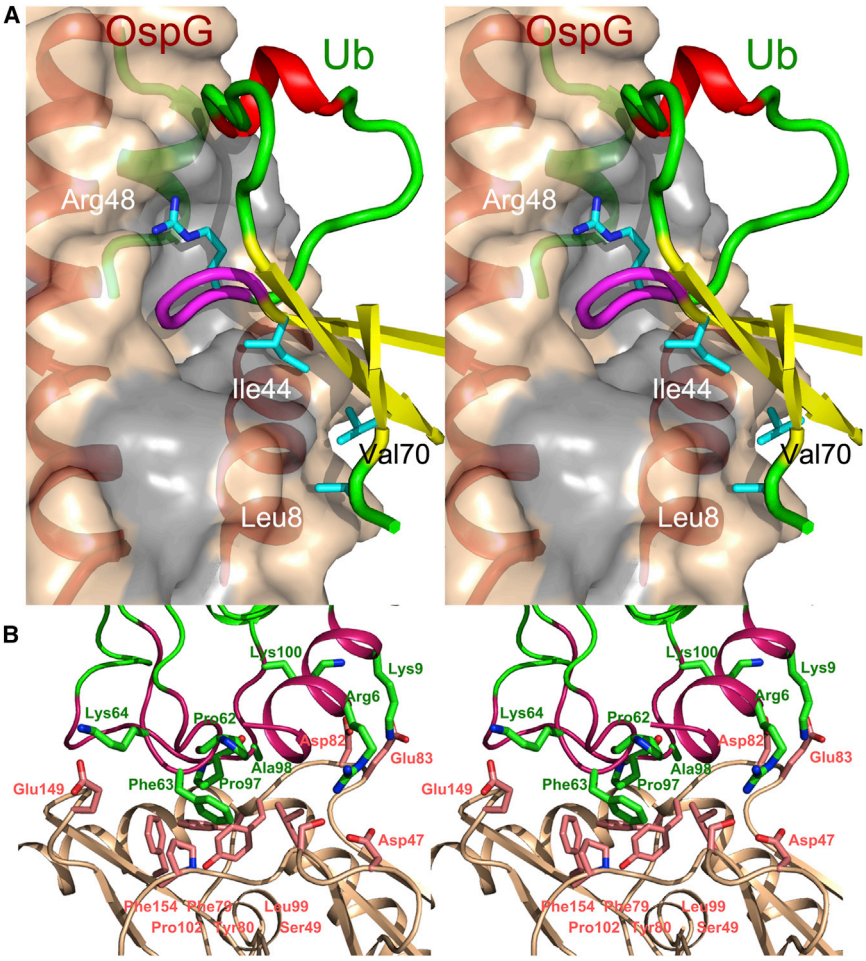

Figure 3. The OspG Interface with UbcH7 and Ub

(A) Surface of OspG, colored gray for hydrophobic residues and wheat elsewhere, with cartoon model of Ub. A deep cavity between the C-terminal helices (α3, α4) of OspG (red) and the "activation loop" (green) is the focal point of the interaction with the β3-β4 turn of Ub (magenta) extending into this cavity. Additional interactions are provided by the short α helix (red) and β strands (yellow) of Ub.

(B) Contacts between OspG (wheat) and UbcH7 (green). The UbcH7 helix (αH1) and two loops (L4, L7) contacting OspG are painted magenta.

Leu99, Pro102, and Phe154), and hydrophilic on the edges (Asp47, Ser49, Asp82, Glu83, Lys128, Glu149, and Ser150) (Figure 3B). This OspG surface is formed by three loops: the loop between α1 (helix C) and β4, the loop following β5, and the turn between hairpin strands β7-β8. The hydrophobic character of this interface in OspG is not present in the structurally closely related NleH kinases (Grishin et al., 2014).

UbcH7 residues in contact with OspG belong to the N-terminal α helix (αH1), loop 4 (L4), and loop 7 (L7) defined for E2s (van Wijk and Timmers, 2010) (Figures 3B and 4). Residues in these regions of UbcH7 are highly conserved among E2s, which might account for the binding of OspG to a number of E2s (Kim et al., 2005). Furthermore, these residues are typically used to recruit RING- and HECT-type E3s (Huang et al., 1999; van Wijk and Timmers, 2010; Budhidarmo et al., 2012). Specifically, the UbcH7 interface with OspG involves a pair of basic residues (Arg5, Arg6) in αH1 and hydrophobic interactions in which Pro62 and Phe63 (L4), and Lys96, Pro97, and Ala98 (L7) contact OspG residues Phe79, Tyr80, Leu99, Pro102, and Phe154. Several hydrogen bonds are also formed at the edges of the interface, including a salt bridge between Arg5 in UbcH7 and Asp47 in OspG.

The structure shows that UbcH7∼Ub bind to two independent sites leaving the active site of OspG accessible not only to ATP but also to potential substrate(s). The covalent connection between UbcH7 and Ub increases the cooperativity between the sites as demonstrated by the 15-fold increased affinity of OspG for UbcH7∼Ub as compared to Ub. However, little interaction between the extended C terminus of Ub and OspG is evident from the structure, indicating that residues involved in the UbcH7∼Ub linkage do not contribute to the binding affinity. The observation that both the E2 and Ub are involved in the recruitment of OspG is reminiscent of the mechanism used by different E2∼Ub conjugates to recruit their cognate E3s. In the OspG:UbcH7∼Ub structure, the Ub in UbcH7∼Ub is disengaged from UbcH7 with a limited contact surface, in agreement with the ^{1}H-^{15}N HSQC spectrum of the UbcH7∼Ub complex showing a limited interaction between the two proteins (Figure S1A). This arrangement is similar to the "open" configuration adopted by UbcH5b∼Ub in complex with NEDD4L, in which Ub is recruited by the C-lobe of the HECT E3 (Kamadurai et al., 2009) (Figure 4). Superposition of the E2∼Ub components in the OspG and NEDD4L complexes shows that the two arrangements are very similar (Figures 4 and S4B). In contrast, comparison of the UbcH7∼Ub configuration with that of UbcH5a-Ub in complex with the RING E3 RNF4 shows little similarity in the Ub positioning. In this structure, the UbcH5a∼Ub adopts a "closed" conformation, in which Ub is in contact with both the E2 and RNF4 (Plechanovová et al., 2012). These observations suggest that OspG might interfere with UbcH7-mediated ubiquitination by recruiting UbcH7∼Ub through a HECT-like structural mimic.

The OspG:UbcH7∼Ub Complex Exhibits Increased Kinase Activity

The structure of the OspG:UbcH7∼Ub complex unequivocally indicates that binding of the UbcH7∼Ub conjugate to OspG does not occlude the kinase active site or the substrate binding site of OspG and should not interfere with the ability of OspG to phosphorylate substrates. It was shown previously that binding of Ub to OspG mildly activates the OspG kinase activity toward histones at 30°C in vitro (Zhou et al., 2013). We investigated the kinase

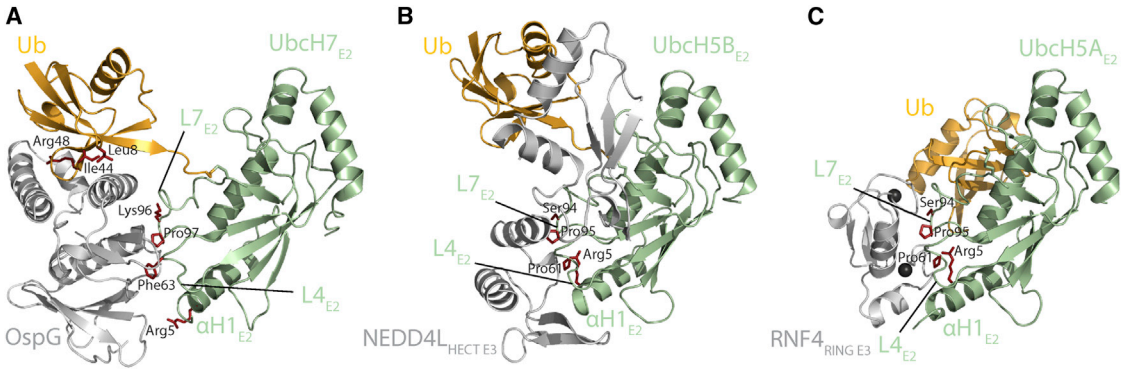

Figure 4. The UbcH7∼Ub Conjugate Adopts an "Open" Conformation upon Binding to OspG

(A) Ribbon diagram showing OspG bound to UbcH7∼Ub. Residues in UbcH7 present in helix αH1 (Arg5) and loops L4 (Phe63) and L7 (Lys96, Pro97) and Ub (Leu8, Ile44 and Arg48) that are important for the interaction with OspG are highlighted in red. The UbcH7∼Ub conjugate is oriented in an "open" conformation.

(B) Ribbon diagram showing UbcH5b∼Ub in the "open" conformation when bound to the HECT E3 NEDD4L (PDB ID code 3JW0) showing residues in helix αH1 and loops L4 and L7 of UbcH5b that are important for the interaction. In NEDD4L, only residues 734–796 and 872–949 are shown for clarity.

(C) Ribbon diagram showing UbcH5a∼Ub in the "closed" conformation when bound to the RING E3 RNF4 (PDB ID code 4AP4). Only residues 131–195 from RNF4 are shown. Panels were prepared by superimposing the E2 structures of UbcH7, UbcH5a, and UbcH5b in PyMOL.

activity of OspG in the presence of the UbcH7∼Ub conjugate or Ub, using histone H1 as a substrate. The presence of Ub stimulated the activity ∼8-fold, whereas the presence of the UbcH7∼Ub conjugate stimulated the activity ∼20-fold (Figure 5). On the other hand, UbcH7 had no effect on OspG activity. These results demonstrated that the kinase activity of OspG was preserved and even largely increased in the OspG:UbcH7∼Ub complex.

UbcH7 Binding to OspG Is Important for Stimulation of the Kinase Activity

Results presented above suggested that binding of both Ub and UbcH7 contribute to OspG activation. Zhou et al. (2013) demonstrated that mutations in the Ub binding site of OspG abolished activation of OspG kinase activity by Ub. To investigate the importance of UbcH7 binding on kinase activation, we constructed the OspG mutants F154R and L99R/P102E affecting residues at the binding surface for UbcH7. In the OspG:UbcH7∼Ub structure, residues L99 and P102 (loop following β5 in the N-lobe) and F154 (β7 in the C-lobe) interact with the L4 and L7 loops of UbcH7 (Figure S4C). As compared to wild-type OspG, the mutants showed similar gel filtration profiles (Figure S5A) and circular dichroism spectra (Figure S5B). The OspG-F154R and OspG- L99R/P102E mutants exhibited a lower kinase activity than did wild-type OspG, and this activity was still stimulated by Ub (Figure 5). In the presence of the UbcH7∼Ub conjugate, only OspG-F154R could be activated, resulting in activity still significantly smaller that the wild-type OspG.

OspG Inhibits the Ubiquitination Activity of the E3 Parkin

In the OspG:UbcH7∼Ub complex, OspG engages UbcH7∼Ub residues involved in the interaction of this UbcH7 with E3s, suggesting that OspG might compete with E3s for the binding to UbcH7 and thereby interfere with the activity of the E3. Furthermore, the dissociation constant (580 nM) of the OspG:UbcH7∼Ub complex reflects a tighter association as compared to the one typically observed for E2-E3 interactions, such as for the interaction of the E3 E6AP with UbcH7∼Ub (dissociation constant of 6.5 μM) (Purbeck et al., 2010) or the E3 parkin with UbcH7 (dissociation constant of 4.7 μM) (Regnström et al., 2013). To investigate whether OspG might inhibit the activity of an E3, we measured the autoubiquitination of the E3 parkin in the presence of E1, UbcH7, Ub, and various amounts of OspG (Figure 6). The presence of OspG led to a strong decrease in the appearance of ubiquitinated parkin molecules and the ubiquitination activity of parkin was almost completely inhibited at an UbcH7:OspG molar ratio of 1:1. To test the importance of the OspG-UbcH7 interaction on the inhibition of the parkin activity by OspG, we used the OspG variants OspG-F154R and OspG-L99R/P102E that impair the interaction between OspG and UbcH7. These OspG variants were unable to inhibit the autoubiquitination activity of parkin (Figure 6). These results indicated that OspG can inhibit the ubiquitination activity of an E3 and that the binding site of UbcH7 onto OspG is necessary for this inhibition.

Recruitment of the UbcH7∼Ub Conjugate Protects OspG from Degradation by the Proteasome

To investigate the contribution of UbcH7 binding onto OspG to the activity of OspG within host cells, plasmids encoding Myc-tagged OspG-WT, OspG-L99R, OspG-P102E, OspG-L99R/P102E, or OspG-F145R were transfected into HEK293T cells. Steady-state amounts of recombinant proteins were analyzed by SDS-PAGE and immunoblotting using anti-Myc antibodies. Unexpectedly, all OspG variants were detected in much lower amounts as compared to wild-type OspG (Figure 7). To investigate whether decreased amounts of OspG variants were due to the increased degradation of these proteins, transfected cells were treated with the proteasome inhibitor MG132 for 3 hr. MG132 treatment led to a slight increase in the amount of wild-type OspG and to a much larger increase in the amounts of all OspG variants (Figure 7). These results strongly suggest that, as compared to wild-type OspG, variants that do not bind UbcH7 have an increased susceptibility to degradation. As a consequence, OspG variants did not prevent phospho-IκBα degradation upon stimulation of transfected cells with TNFα to induce the NF-κB pathway (data not shown).

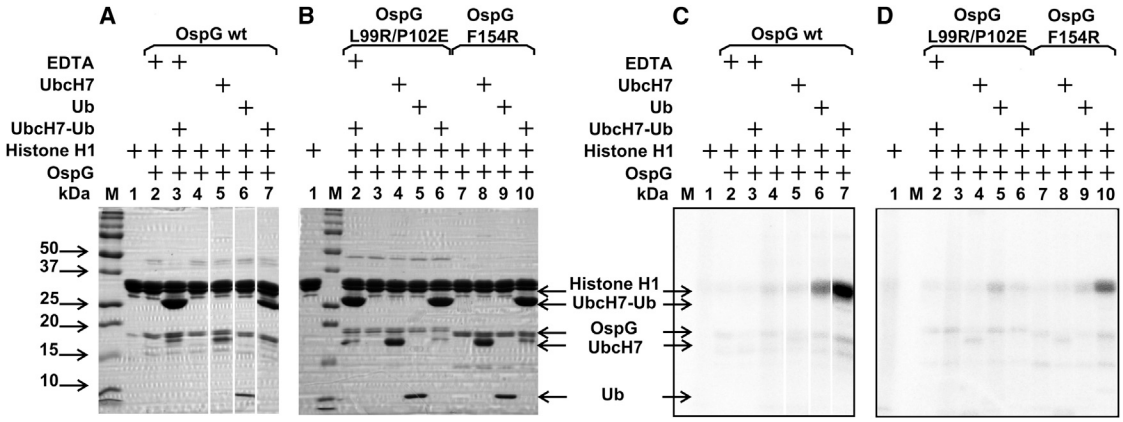

Figure 5. Activity and Activation of OspG and OspG Mutants at 28°C Using [γ-^{32}P]ATP

(A) The nonreducing SDS-PAGE for OspG. Lanes: 1, histone H1 (5 μg); 2, histone H1 (5 μg) + OspG (1.3 μg), EDTA; 3, histone H1 (5 μg) + UbcH7-Ub (5.4 μg) + OspG (1.3 μg), EDTA; 4, histone H1 (5 μg) + OspG (1.3 μg); 5, histone H1 (5 μg) + UbcH7 (1.2 μg) + OspG (1.3 μg); 6, histone H1 (5 μg) + Ub (0.56 μg) + OspG (1.3 μg); 7, histone H1 (5 μg) + UbcH7-Ub (1.8 μg) + OspG (1.3 μg).

(B) The nonreducing SDS-PAGE for OspG(L99R/P102E) and OspG(F154R) mutants. Lanes: 1, histone H1 (5 μg); 2, histone H1 (5 μg) + UbcH7-Ub (5.4 μg) + OspG(L99R/P102E) (1.3 μg), EDTA; 3, histone H1 (5 μg) + OspG(L99R/P102E) (1.3 μg); 4, histone H1 (5 μg) + UbcH7 (3.6 μg) + OspG(L99R/P102E) (1.3 μg); 5, histone H1 (5 μg) + Ub (1.7 μg) + OspG(L99R/P102E) (1.3 μg); 6, histone H1 (5 μg) + UbcH7-Ub (5.4 μg) + OspG(L99R/P102E) (1.3 μg); 7, histone H1 (5 μg) + OspG(F154R) (1.3 μg); 8, histone H1 (5 μg) + UbcH7 (3.6 μg) + OspG(F154R) (1.3 μg); 9, histone H1 (5 μg) + Ub (1.7 μg) + OspG(F154R) (1.3 μg); 10, histone H1 (5 μg) + UbcH7-Ub (5.4 μg) + OspG(F154R) (1.3 μg).

(C) Radioscan of the gel in (A).

(D) Radioscan of the gel in (B).

DISCUSSION

The OspG kinase is one of ∼20 *Shigella* effectors contributing to host invasion and subversion of cellular functions. One of the effects of OspG is to dampen activation of the NF-κB pathway by preventing the degradation of phospho-IκBα; however, the sequence of events leading to this effect is not elucidated. OspG was shown to bind a number of E2s and to associate preferentially to E2∼Ub conjugates, rather than to E2s alone (Kim et al., 2005). In addition, OspG binding to Ub and poly-Ub chains has been reported (Zhou et al., 2013), and the kinase activity of OspG (Kim et al., 2005) was shown to be stimulated by Ub (Zhou et al., 2013). Results presented therein on the association of OspG with an UbcH7∼Ub conjugate, the increased kinase activity of the complex, and the inhibitory effect of OspG on the activity of the E3 parkin, together with the elucidation of the structure of the OspG:UbcH7∼Ub complex, shed light on the mode of action of this effector.

OspG does not conform to typical eukaryotic kinases (Kannan et al., 2007) and is structurally most closely related to Rio (Laronde-Leblanc et al., 2005) and Bud32 (Hecker et al., 2008) atypical kinases. It contains only the most basic elements of the kinase fold and is much smaller than typical regulatory kinases. Although the shorter "activation loop" of OspG contains three Tyr residues and one Thr residue, these residues are either facing away from the active site or are located too far away to provide an effective regulation of the kinase activity by phosphorylation. Indeed, the conformation of OspG in the OspG:UbcH7∼Ub complex closely resembles the active conformation of regulatory kinases.

Considering the active site as the front of OspG, binding of UbcH7∼Ub involves the side and back surfaces of OspG, leaving the active site accessible for potential substrates. The interface with Ub is centered on a deep depression formed between α3 and α4 of OspG and engages two regions of Ub surrounding residues Ile44 and Tyr59. The former is known to participate in Ub binding to other proteins (Beal et al., 1998; Sloper-Mould et al., 2001; Lee et al., 2006). Comparison with the structure of PKA indicates that the displacement of the N-terminal end of α4 in OspG is crucial for the formation of the Ub binding depression. Zhou et al. (2013) showed that mutations L190D/L191D abolished Ub binding and proposed that these residues interact with the Ile44 patch on Ub. However, the structure of OspG:UbcH7∼Ub indicates that these two Leu residues are located at the last turn of α3; they are not in contact with Ub, but rather face the interior of the molecule and interact with hydrophobic residues in α2. Their replacement by acidic residues might cause a readjustment of α2 and α3, thereby distorting the Ub binding interface of OspG. UbcH7 interacts with OspG through a surface encompassing residues in L4 (Pro62, Phe63) and L7 (Lys96, Pro97, Ala98) of UbcH7. Upon interaction with OspG, UbcH7∼Ub adopts an "open" conformation similar to the one observed for UbcH5b-Ub interacting with the HECT E3 ligase NEDD4L (Kamadurai et al., 2009). Both the 3D structure and affinity measurements of OspG for UbcH7∼Ub, UbcH7, and Ub suggest that the E2∼Ub conjugate might be the most relevant partner of OspG within host cells.

We confirmed that the kinase activity of OspG is enhanced in the presence of Ub (Zhou et al., 2013) and showed that this activity is even more stimulated in the presence of the UbcH7∼Ub conjugate. To investigate the respective contributions of UbcH7 and Ub binding to OspG on the stimulation of the kinase activity, we used the OspG variants L99R/P102E and F154R altered in the UbcH7 binding site. The circular

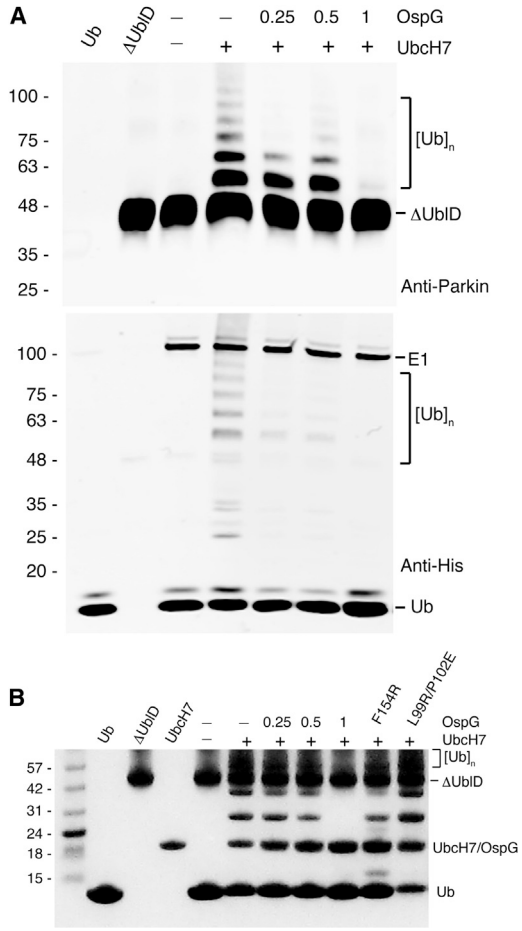

Figure 6. Inhibition of Parkin Activity by OspG

(A) Western blot analysis of autoubiquitination assays of ΔUblD parkin using anti-parkin (top) and anti-His (bottom) antibodies from 4%–15% SDS PAGE. On each blot, the first two lanes contain either Ub (Ub) or parkin (ΔUblD) alone. All other lanes contain E1, ATP, and reactants indicated above the lanes. Amounts of OspG are equivalents relative to UbcH7. Autoubiquitination products $[Ub]_n$ detected using anti-parkin or anti-His (recognizing His-Ub) antibodies are indicated.

(B) Coomassie-stained 8% Bis-Tris SDS PAGE as described in (A).

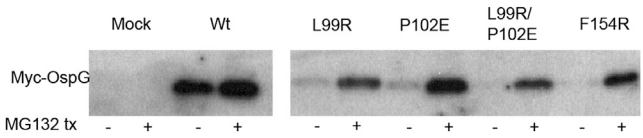

Figure 7. Expression of Wild-Type and Variant OspG Proteins in Transfected HEK293T Cells

Cells transfected by pRK5-myc (vector) or pRK5-myc-OspG-encoding wild-type OspG (WT) or its derivatives harboring the indicated replacements were (+) or not (–) treated with the proteasome inhibitor MG132 (MG132 tx). After 3 hr, samples were analyzed by SDS-PAGE and immunoblotting using a serum raised against the Myc tag.

dichroism spectra (Figure S5B) of these two variants were similar to that of wild-type OspG, suggesting that the structure of the soluble proteins was not affected by these replacements; as in the case of wild-type OspG, their activity was increased in the presence of Ub. The effect of the UbcH7∼Ub conjugate on the activity of the L99R/P102E mutant was reduced to the one observed with Ub, indicating that the UbcH7 binding site on OspG was indeed disrupted in this variant. Stimulation of the kinase activity of the OspG-F154R mutant by UbcH7∼Ub was intermediate between wild-type OspG and OspG-L99R/P102E, suggesting that this mutant was still able to interact with the UbcH7 moiety of the conjugate, albeit less strongly than wild-type OspG. Indeed, Phe154 of OspG stacks against Phe63 of UbcH7, and it is possible that the aliphatic side chain of the Arg residue in F154R mutant can still provide an interactive surface for Phe63 in UbcH7. These results are evidence that binding of the UbcH7 moiety in the UbcH7∼Ub conjugate is essential for the full stimulation of the kinase activity of OspG. The Ub binding surface on OspG is away from the kinase active site, and the structure of the OspG:UbcH7∼Ub complex provides no direct explanations for activation of OspG by Ub or the UbcH7∼Ub conjugate. However, considering the effect of OspG mutations, it seems likely that structural changes might occur in OspG upon binding of the UbcH7∼Ub conjugate (or Ub). The conformation of OspG in solution would not be catalytically active, and an adjustment in the relative orientations of the N- and C-terminal lobes might have to occur to get the active form observed in the crystal structure. Indeed, in the structure of the OspG:UbcH7∼Ub complex, OspG is in an active conformation and binds the nucleotide without any further conformational adjustment. Insertion of the turn located between β3 and β4 of Ub into the depression in OspG surface (Figure 3A) might be involved in the spatial reorganization of the catalytic site upon binding of UbcH7∼Ub.

Residues of UbcH7 interacting with OspG are conserved in various E2s and are involved in the interaction of E2s with their E3 partners (Budhidarmo et al., 2012). This observation suggested that OspG might interfere with the activity of E3s by competing with E3s for the recruitment of E2-Ub conjugates. Indeed, at a 1:1 molar ratio of OspG:UbcH7, the autoubiquitination activity of parkin was strongly inhibited. Furthermore, the effects of the replacements F154R and L99R/P102E on the inhibition of parkin activity mirrored the effects these replacements had on the stimulation of the kinase activity of OspG, i.e., a partial effect for F154R and a complete loss for L99R/P102E. Transfection of human cells by plasmids expressing wild-type OspG and variants affected in the UbcH7 binding site showed that these variants were degraded more rapidly than wild-type OspG. This result suggests that OspG in its monomeric form is more prone to degradation than in its UbcH7∼Ub-associated form and that binding of the E2∼Ub conjugate stabilizes OspG in the intracellular environment. The difference in viability of OspG associated or not with E2∼Ub in the intracellular environment supports the above proposal that OspG might exist in two conformations. Because of their premature degradation, OspG variants unable to bind UbcH7 did not prevent phospho-IκBα degradation upon stimulation of transfected cells with TNFα.

In conclusion, we showed that (1) the E2∼Ub conjugate is the likely biological partner of OspG, because the affinity of OspG to the conjugate is much higher than the affinity to Ub alone; (2) binding of UbcH7∼Ub involves two nonoverlapping surfaces

on OspG and, in this complex, the OspG active site is accessible to potential substrates; (3) binding of UbcH7∼Ub increases the kinase activity of OspG, possibly by stabilizing a more active conformation that is also less prone to degradation in the intracellular environment; and (4) Kim et al. (2005) proposed that the E2∼Ub conjugate was used by OspG as a "delivery vehicle" to be targeted to and phosphorylate the E3 $SCF^{\beta\text{-}TrCP}$ complex involved in phospho-IκB ubiquitination (Yaron et al., 1998). However, this mode of action appears unlikely because the region of the E2 binding to the E3 $SCF^{\beta\text{-}TrCP}$ complex (Zheng et al., 2002) is the same that binds to OspG and, as shown here for the E3 parkin, OspG, and $SCF^{\beta\text{-}TrCP}$ would compete for E2∼Ub conjugates. The present discovery that the E2 engages with OspG through a surface that is similar to that used for its interaction with both the E1 and the E3s indicates that OspG interferes in the ubiquitination process, at least in part, by hijacking E2∼Ub.

EXPERIMENTAL PROCEDURES

Cloning, Mutagenesis, and Protein Expression

The portion of the *Shigella flexneri* 2a strain 2457T *ospG* gene-encoding residues 26–196 was inserted into pMCSG7 (pET21-derivative) using the ligase independent cloning (LIC) procedure adding a TEV-cleavable His_6-tag. Ub(K48R/G76C) and UbcH7(C17S/C137S) were expressed as previously described (Merkley et al., 2005; Serniwka and Shaw, 2009). All constructs were transformed into BL21(DE3)Star (Invitrogen) or BL21(DE3) (Novagen) cells; bacteria were grown in Terrific broth at 37°C until the OD_{600} reached 0.6 units. Expression was induced with 1 mM isopropyl β-D-1-thiogalactopyranoside for 12–16 hr at 20°C. For ^{15}N-labeled proteins, cells were grown in M9 media using $^{15}NH_4Cl$ as the sole nitrogen source as previously described (Merkley et al., 2005; Serniwka and Shaw, 2009).

Mutations corresponding to F154R and L99R/P102E were introduced using the QuikChange mutagenesis scheme, yielding OspG-154R and OspG-L99R/P102E. The Phe154 codon *TTC* was replaced by the Arg codon *CGC*; the Leu99 codon *CTG* was replaced by the Arg codon *CGG*; and the Pro102 codon *CCT* was replaced by the Glu codon *GAA*.

Protein Purification and UbcH7∼Ub Conjugation

Details for the purification of Ub and UbcH7 have been previously described (Merkley et al., 2005; Serniwka and Shaw, 2009). The UbcH7∼Ub conjugate was obtained following the procedure by Merkley et al. (2005), where the natural thioester bond between Cys86 in UbcH7 and the carboxylic group of Gly76 in Ub was replaced by a disulfide bond. To this end, the UbcH7∼Ub conjugate was formed between UbcH7(C17S/C137S) and Ub(K48R/G76C) proteins via mild Cu^{2+} oxidation (Figures S5C and S5D).

After purification on Ni-NTA beads (QIAGEN), OspG was dialyzed overnight against 50 mM HEPES and 50 mM NaCl at pH 8.0. The His_6-tag was cleaved with TEV protease using a 30:1 (w/w) ratio and 2 hr incubation at 28°C. TEV protease and uncleaved OspG were removed by reapplication to Ni-NTA beads. The cleaved OspG was purified through gel-filtration on a Superdex 75 10/300 (GE Healthcare) in 15 mM HEPES, 50 mM NaCl at pH 8.0 with or without 0.5 mM TCEP. OspG mutants were expressed and purified in the same way as the wild-type OspG. OspG wild-type was characterized under reducing conditions by size-exclusion chromatography and dynamic light scattering. Both methods showed that OspG is monomeric in solution (Figure S5E). However, in the absence of reducing agent, we also observed the presence of dimeric disulfide-bridged species (via Cys127; Figure S5E). The crystallization was conducted under nonreducing conditions by mixing the purified UbcH7∼Ub conjugate with the monomeric OspG fraction from gel filtration performed under nonreducing conditions. The OspG F154R and L99R/P102E mutants produced sharp peaks on gel filtration at the elution volume similar to the wild-type OspG (Figure S5A).

Monomeric OspG was incubated with UbcH7∼Ub (molar ratio 1:1) and purified using gel filtration on Superdex 75 in the same buffer. The formation of the OspG:UbcH7∼Ub complex was monitored by gel filtration. The effect of disulfide bond formation on the complex stability was investigated by treating the mixture with 5 mM DTT for 15 min and followed with gel filtration on Superdex 75 (Figure S2). For other interaction experiments, OspG was purified in the presence of 0.5 mM TCEP.

NMR Spectroscopy

All NMR experiments were collected on a 600 MHz Varian Inova spectrometer (Biomolecular NMR Facility, University of Western Ontario) equipped with a triple-resonance probe and x,y,z gradients. ^1H-^{15}N HSQC spectra were acquired using the sensitivity-enhanced method at 25°C (Barbato et al., 1992). All samples were prepared in 100 mM NaH_2PO4, 100 mM NaCl at pH 7.5 and contained ^{15}N-labeled Ub, ^{15}N-labeled UbcH7, or UbcH7∼Ub in which only the UbcH7 moiety was ^{15}N-labeled. Assignments for these proteins have been previously reported (Hamilton et al., 2000; Serniwka and Shaw, 2008). For protein interaction experiments, duplicate samples were made of the ^{15}N-labeled protein (100 μM) in the absence and presence of OspG (200 μM). Samples were then mixed to obtain intermediate ratios. All spectral parameters used to collect data of a particular ^{15}N-labeled protein ± OspG were identical. Samples were referenced directly to a DSS internal standard. Data were processed using 60°-shifted cosine bell-weighting functions in the ^1H and ^{15}N dimensions using NMRPipe (Delaglio et al., 1995) and analyzed using NMRView (Johnson and Blevins, 1994).

Isothermal Titration Calorimetry

All calorimetry experiments were done using a Microcal VP-ITC system (GE Healthcare) using freshly prepared proteins in 100 mM NaH_2PO_4, 100 mM NaCl at pH 7.5. UbcH7, Ub, or UbcH7∼Ub proteins were titrated into the calorimeter cell containing OspG. Protein concentrations were determined using amino acid analysis (SPARC BioCentre Amino Acid Facility). All experiments were completed in triplicate at 25°C, and data were analyzed using a single-site binding model in Origin (OriginLab).

Protein Crystallization

Purified OspG:UbcH7∼Ub complex was concentrated to 14 mg/ml, and aliquots were mixed with 5 mM AMPPNP and Mg^{2+}. Initial crystals were obtained by the sitting drop method with ProComplex solutions (QIAGEN). The best crystals were obtained from 0.1 M $MgCl_2$, 0.1 M HEPES, and 15% PEG 4000 at pH 8.0 and were cryoprotected in 0.1 M $MgCl_2$, 0.1 M HEPES, 15% PEG 4000, and 25% glycerol at pH 8.0. Attempts to obtain crystals of free OspG were not successful.

Structure Determination

Diffraction data were collected at the CMCF-ID beamline at the Canadian Light Source. Data were integrated and scaled with HKL3000 (Minor et al., 2006) (Table 1). The structure was solved by molecular replacement with Phaser (McCoy et al., 2007) using the UbcH7 structure first (PDB ID code 3SY2, chain C) (Lin et al., 2012), then the NleH2 structure (PDB ID code 4LRK), and next the Ub structure (PDB ID code 2KJH, chain B) (Serniwka and Shaw, 2009). Phenix_refine (Adams et al., 2011) and Coot (Emsley et al., 2010) were used for iterative model refining and rebuilding. The pertinent details are shown in Table 1.

Circular Dichroism

The circular dichroism spectra for OspG-WT, OspG-F154R, and OspG-L99R/P102E were recorded using AppliedPhotophysics Chirascan-plus Circular Dichroism Spectrometer. Prior to the assay, proteins were dialyzed against 10 mM Na-phosphate buffer (pH 7.5). The spectra were recorded in the range of 180–260 nm at a protein concentration of 75 μg/ml.

In Vitro Kinase Activity Measurements

We measured the kinase activity of OspG in vitro with [γ-32P]ATP and histones as an exogenous substrate using a modified protocol of Zhou et al. (2013). The solution of OspG was dialyzed overnight against the reaction buffer to ensure the absence of DTT in the sample. The 10 μl reaction mixtures contained 1.3 μg of OspG and 5 μg of histone H1 preparation (Millipore) in 25 mM Tris-HCl (pH 7.5), 10 mM $MgCl_2$. Additionally 0.56 μg of Ub or 1.2 μg of UbcH7 or 1.8 μg of UbcH7-Ub were added to the reaction mixture, providing the final 1:1 molar ratio with OspG. In the case of OspG mutants, which showed reduced

activity, 1.3 μg of OspG was premixed with 1.7 μg of Ub, 3.6 μg of UbcH7 or 5.4 μg of UbcH7-Ub, increasing the OspG-to-binding partner molar ratio to 1:3. The reactions were carried out for 1 hr at 28°C and were started by addition of a mixture of "cold" ATP with [γ-32P]ATP to a final concentration of 100 μM ATP and 2 μCi/reaction of [γ-32P]ATP (3,000 Ci/mmol). Phosphorylation was monitored by imaging the radiolabeled proteins on nonreducing SDS-PAGE using Molecular Imager FX phosphorimager (Bio-Rad). The control was the sample containing histone H1, OspG, UbcH7-Ub, and 10 mM EDTA instead of Mg^{2+}.

Ubiquitin Ligase Inhibition Assay

The ability of OspG to inhibit Ub transfer from E2 to E3 was monitored using an autoubiquitination assay. Briefly, the ubiquitination of the C-terminal portion of the human E3 ligase parkin (residues 77–465; ΔUblD) was monitored following the published protocol (Chaugule et al., 2011) with some modifications. A series of 25 μL reactions were set up using human recombinant E1 (15 nM), UbcH7 (0.5 uM), His-tagged ubiquitin (5 uM), ΔUblD (1 μM), and 0–1 μM OspG. A buffer containing 50 mM HEPES (pH 7.5), 5 mM $MgCl_2$, and 5 mM ATP was used. Reactions were incubated at 37°C for 1 hr prior to quenching with SDS-loading buffer containing DTT. Samples were run on 4%–15% tris-glycine gels and transferred to polyvinylidene fluoride membranes. After treatment with primary and secondary antibodies, the blots were imaged using an Odyssey imaging instrument (LI-COR Biosciences) at 700 nm. Anti-His antibodies were a generous gift from Dr. D. Litchfield (UWO). IRDye 680RD Goat anti-Rabbit immunoglobulin G was from LI-COR Biosciences.

Expression of OspG in HEK293T Cells

The *ospG* coding sequence was previously cloned in the vector pRK5-Myc for expression of OspG with an Myc-tag fused to its N terminus (Kim et al., 2005). Mutations were introduced into the plasmid pRK5-myc-OspG to encode OspG variants with L99R, P102E, L99R/P102E, and F154R replacements. HEK293T cells were plated at 5×10^4 cells/well of a 12-well plate. Approximately 20 hr later, cells were transfected with 0.8 μg of pRK5-Myc (vector), pRK5-Myc-OspG (WT OspG), or its derivatives encoding OspG variants using Attractene transfection reagent (QIAGEN). At 40 hr posttransfection, cells were, or not, treated with 10 μM MG132 (Sigma-Aldrich) for 3 hr. Samples were recovered directly from plates in the reducing Laemli loading buffer (2×), boiled for 5 min, and sonicated during 10 s to shear the DNA. Samples were loaded on 4%–20% gradient miniprotean gels (Bio-Rad) and analyzed by immunoblotting using a polyclonal serum directed against the Myc epitope (Santa Cruz, ref. sc-789).

ACCESSION NUMBERS

The Protein Data Bank ID codes for the coordinates and structure factors reported in this paper are 4Q5E for the OspG+UbcH7∼Ub complex and 4Q5H for the OspG+UbcH7∼Ub+AMPPNP complex.

SUPPLEMENTAL INFORMATION

Supplemental Information includes five figures and can be found with this article online at http://dx.doi.org/10.1016/j.str.2014.04.010.

AUTHOR CONTRIBUTIONS

A.M.G., G.S.S., C.P., and M.C. conceived and designed the experiments. A.M.G., T.E.C.C., K.R.B., and F.-X.C.-V. performed the experiments. A.M.G., T.E.C.C., K.R.B., G.S.S., and M.C. analyzed the data. A.M.G., G.S.S., and M.C. wrote the paper.

ACKNOWLEDGMENTS

We would like to thank Dr. D. Anderson and Ms. D. Detillieux for their help with the radioactive kinase assays. This work was supported by grants from the Canadian Institutes of Health Research (CIHR) (MOP-48370 to M.C. and MOP-14606 to G.S.S.), the Canadian Foundation for Innovation (to M.C.), and by a CIHR training related to synchrotron techniques (CIHR-TRUST) fellowship (to A.M.G.). Diffraction data were collected at the beamline 08ID-1 at the Canadian Light Source, which is supported by the National Science and Engineering Research Council, the National Research Council Canada, CIHR, the Province of Saskatchewan, Western Economic Diversification Canada, and the University of Saskatchewan.

Received: December 14, 2013
Revised: March 19, 2014
Accepted: April 9, 2014
Published: May 22, 2014

REFERENCES

Adams, P.D., Afonine, P.V., Bunkóczi, G., Chen, V.B., Echols, N., Headd, J.J., Hung, L.W., Jain, S., Kapral, G.J., Grosse Kunstleve, R.W., et al. (2011). The Phenix software for automated determination of macromolecular structures. Methods *55*, 94–106.

Barbato, G., Ikura, M., Kay, L.E., Pastor, R.W., and Bax, A. (1992). Backbone dynamics of calmodulin studied by 15N relaxation using inverse detected two-dimensional NMR spectroscopy: the central helix is flexible. Biochemistry *31*, 5269–5278.

Beal, R.E., Toscano-Cantaffa, D., Young, P., Rechsteiner, M., and Pickart, C.M. (1998). The hydrophobic effect contributes to polyubiquitin chain recognition. Biochemistry *37*, 2925–2934.

Buchrieser, C., Glaser, P., Rusniok, C., Nedjari, H., D'Hauteville, H., Kunst, F., Sansonetti, P., and Parsot, C. (2000). The virulence plasmid pWR100 and the repertoire of proteins secreted by the type III secretion apparatus of Shigella flexneri. Mol. Microbiol. *38*, 760–771.

Budhidarmo, R., Nakatani, Y., and Day, C.L. (2012). RINGs hold the key to ubiquitin transfer. Trends Biochem. Sci. *37*, 58–65.

Chaugule, V.K., Burchell, L., Barber, K.R., Sidhu, A., Leslie, S.J., Shaw, G.S., and Walden, H. (2011). Autoregulation of Parkin activity through its ubiquitin-like domain. EMBO J. *30*, 2853–2867.

Dean, P. (2011). Functional domains and motifs of bacterial type III effector proteins and their roles in infection. FEMS Microbiol. Rev. *35*, 1100–1125.

Delaglio, F., Grzesiek, S., Vuister, G.W., Zhu, G., Pfeifer, J., and Bax, A. (1995). NMRPipe: a multidimensional spectral processing system based on UNIX pipes. J. Biomol. NMR *6*, 277–293.

Dou, H., Buetow, L., Sibbet, G.J., Cameron, K., and Huang, D.T. (2012). BIRC7-E2 ubiquitin conjugate structure reveals the mechanism of ubiquitin transfer by a RING dimer. Nat. Struct. Mol. Biol. *19*, 876–883.

Emsley, P., Lohkamp, B., Scott, W.G., and Cowtan, K. (2010). Features and development of Coot. Acta Crystallogr. D Biol. Crystallogr. *66*, 486–501.

Gao, X., Wan, F., Mateo, K., Callegari, E., Wang, D., Deng, W., Puente, J., Li, F., Chaussee, M.S., Finlay, B.B., et al. (2009). Bacterial effector binding to ribosomal protein s3 subverts NF-kappaB function. PLoS Pathog. *5*, e1000708.

Ge, J., Xu, H., Li, T., Zhou, Y., Zhang, Z., Li, S., Liu, L., and Shao, F. (2009). A Legionella type IV effector activates the NF-kappaB pathway by phosphorylating the IkappaB family of inhibitors. Proc. Natl. Acad. Sci. USA *106*, 13725–13730.

Grishin, A.M., Cherney, M., Anderson, D.H., Phanse, S., Babu, M., and Cygler, M. (2014). NleH defines a new family of bacterial effector kinases. Structure *22*, 250–259.

Hamilton, K.S., Ellison, M.J., and Shaw, G.S. (2000). Letter to the editor: 1H, 15N and 13C resonance assignments for the catalytic domain of the yeast E2, UBC1. J. Biomol. NMR *16*, 351–352.

Hanks, S.K., and Hunter, T. (1995). Protein kinases 6. The eukaryotic protein kinase superfamily: kinase (catalytic) domain structure and classification. FASEB J. *9*, 576–596.

Hecker, A., Lopreiato, R., Graille, M., Collinet, B., Forterre, P., Libri, D., and van Tilbeurgh, H. (2008). Structure of the archaeal Kae1/Bud32 fusion protein MJ1130: a model for the eukaryotic EKC/KEOPS subcomplex. EMBO J. *27*, 2340–2351.

Huang, L., Kinnucan, E., Wang, G., Beaudenon, S., Howley, P.M., Huibregtse, J.M., and Pavletich, N.P. (1999). Structure of an E6AP-UbcH7 complex:

insights into ubiquitination by the E2-E3 enzyme cascade. Science *286*, 1321–1326.

Johnson, B.A., and Blevins, R.A. (1994). NMR View: A computer program for the visualization and analysis of NMR data. J. Biomol. NMR *4*, 603–614.

Kamadurai, H.B., Souphron, J., Scott, D.C., Duda, D.M., Miller, D.J., Stringer, D., Piper, R.C., and Schulman, B.A. (2009). Insights into ubiquitin transfer cascades from a structure of a UbcH5B approximately ubiquitin-HECT(NEDD4L) complex. Mol. Cell *36*, 1095–1102.

Kannan, N., Taylor, S.S., Zhai, Y., Venter, J.C., and Manning, G. (2007). Structural and functional diversity of the microbial kinome. PLoS Biol. *5*, e17.

Kim, D.W., Lenzen, G., Page, A.L., Legrain, P., Sansonetti, P.J., and Parsot, C. (2005). The Shigella flexneri effector OspG interferes with innate immune responses by targeting ubiquitin-conjugating enzymes. Proc. Natl. Acad. Sci. USA *102*, 14046–14051.

Kornev, A.P., Haste, N.M., Taylor, S.S., and Eyck, L.F. (2006). Surface comparison of active and inactive protein kinases identifies a conserved activation mechanism. Proc. Natl. Acad. Sci. USA *103*, 17783–17788.

Kornev, A.P., Taylor, S.S., and Ten Eyck, L.F. (2008). A helix scaffold for the assembly of active protein kinases. Proc. Natl. Acad. Sci. USA *105*, 14377–14382.

Laronde-Leblanc, N., Guszczynski, T., Copeland, T., and Wlodawer, A. (2005). Structure and activity of the atypical serine kinase Rio1. FEBS J. *272*, 3698–3713.

Lee, S., Tsai, Y.C., Mattera, R., Smith, W.J., Kostelansky, M.S., Weissman, A.M., Bonifacino, J.S., and Hurley, J.H. (2006). Structural basis for ubiquitin recognition and autoubiquitination by Rabex-5. Nat. Struct. Mol. Biol. *13*, 264–271.

Lin, D.Y., Diao, J., and Chen, J. (2012). Crystal structures of two bacterial HECT-like E3 ligases in complex with a human E2 reveal atomic details of pathogen-host interactions. Proc. Natl. Acad. Sci. USA *109*, 1925–1930.

Manning, G., Whyte, D.B., Martinez, R., Hunter, T., and Sudarsanam, S. (2002). The protein kinase complement of the human genome. Science *298*, 1912–1934.

Matsumoto, H., and Young, G.M. (2006). Proteomic and functional analysis of the suite of Ysp proteins exported by the Ysa type III secretion system of Yersinia enterocolitica Biovar 1B. Mol. Microbiol. *59*, 689–706.

McCoy, A.J., Grosse-Kunstleve, R.W., Adams, P.D., Winn, M.D., Storoni, L.C., and Read, R.J. (2007). Phaser crystallographic software. J. Appl. Cryst. *40*, 658–674.

Merkley, N., Barber, K.R., and Shaw, G.S. (2005). Ubiquitin manipulation by an E2 conjugating enzyme using a novel covalent intermediate. J. Biol. Chem. *280*, 31732–31738.

Minor, W., Cymbrowski, M., Otwinowski, Z., and Chruszcz, M. (2006). HKL-3000: the integration of data reduction and structure solution–from diffraction images to an initial model in minutes. Acta Crystallogr. *D62*, 859–866.

Page, R.C., Pruneda, J.N., Amick, J., Klevit, R.E., and Misra, S. (2012). Structural insights into the conformation and oligomerization of E2∼ubiquitin conjugates. Biochemistry *51*, 4175–4187.

Plechanovová, A., Jaffray, E.G., Tatham, M.H., Naismith, J.H., and Hay, R.T. (2012). Structure of a RING E3 ligase and ubiquitin-loaded E2 primed for catalysis. Nature *489*, 115–120.

Poh, J., Odendall, C., Spanos, A., Boyle, C., Liu, M., Freemont, P., and Holden, D.W. (2008). SteC is a Salmonella kinase required for SPI-2-dependent F-actin remodelling. Cell. Microbiol. *10*, 20–30.

Purbeck, C., Eletr, Z.M., and Kuhlman, B. (2010). Kinetics of the transfer of ubiquitin from UbcH7 to E6AP. Biochemistry *49*, 1361–1363.

Regnström, K., Yan, J., Nguyen, L., Callaway, K., Yang, Y., Diep, L., Xing, W., Adhikari, A., Beroza, P., Hom, R.K., et al. (2013). Label free fragment screening using surface plasmon resonance as a tool for fragment finding - analyzing parkin, a difficult CNS target. PLoS ONE *8*, e66879.

Serniwka, S.A., and Shaw, G.S. (2008). 1H, 13C and 15N resonance assignments for the human E2 conjugating enzyme, UbcH7. Biomol. NMR Assign. *2*, 21–23.

Serniwka, S.A., and Shaw, G.S. (2009). The structure of the UbcH8-ubiquitin complex shows a unique ubiquitin interaction site. Biochemistry *48*, 12169–12179.

Sloper-Mould, K.E., Jemc, J.C., Pickart, C.M., and Hicke, L. (2001). Distinct functional surface regions on ubiquitin. J. Biol. Chem. *276*, 30483–30489.

van Wijk, S.J.L., and Timmers, H.T.M. (2010). The family of ubiquitin-conjugating enzymes (E2s): deciding between life and death of proteins. FASEB J. *24*, 981–993.

Wenzel, D.M., Lissounov, A., Brzovic, P.S., and Klevit, R.E. (2011). UBCH7 reactivity profile reveals parkin and HHARI to be RING/HECT hybrids. Nature *474*, 105–108.

Wiley, D.J., Shrestha, N., Yang, J., Atis, N., Dayton, K., and Schesser, K. (2009). The activities of the Yersinia protein kinase A (YpkA) and outer protein J (YopJ) virulence factors converge on an eIF2alpha kinase. J. Biol. Chem. *284*, 24744–24753.

Worrall, L.J., Lameignere, E., and Strynadka, N.C. (2011). Structural overview of the bacterial injectisome. Curr. Opin. Microbiol. *14*, 3–8.

Yaron, A., Hatzubai, A., Davis, M., Lavon, I., Amit, S., Manning, A.M., Andersen, J.S., Mann, M., Mercurio, F., and Ben-Neriah, Y. (1998). Identification of the receptor component of the IkappaBalpha-ubiquitin ligase. Nature *396*, 590–594.

Zheng, N., Schulman, B.A., Song, L., Miller, J.J., Jeffrey, P.D., Wang, P., Chu, C., Koepp, D.M., Elledge, S.J., Pagano, M., et al. (2002). Structure of the Cul1-Rbx1-Skp1-F boxSkp2 SCF ubiquitin ligase complex. Nature *416*, 703–709.

Zhou, Y., Dong, N., Hu, L., and Shao, F. (2013). The Shigella type three secretion system effector OspG directly and specifically binds to host ubiquitin for activation. PLoS ONE *8*, e57558.

